Free Radical Biology & Medicine 52 (2012) 357–365

Contents lists available at SciVerse ScienceDirect

Free Radical Biology & Medicine

journal homepage: www.elsevier.com/locate/freeradbiomed

Original Contribution

NAD(P)H oxidase-dependent intracellular and extracellular $O_2^{\bullet-}$ production in coronary arterial myocytes from CD38 knockout mice

Ming Xu, Yang Zhang, Min Xia, Xiao-Xue Li, Joseph K. Ritter, Fan Zhang, Pin-Lan Li *

Department of Pharmacology and Toxicology, Medical College of Virginia, Virginia Commonwealth University, Richmond, VA 23298, USA

ARTICLE INFO

Article history:
Received 23 June 2011
Revised 20 October 2011
Accepted 24 October 2011
Available online 3 November 2011

Keywords:
ADP-ribose
Ca^{2+}
Redox signaling
Artery
Vasoconstriction
Coronary circulation
Free radicals

ABSTRACT

Activation of NAD(P)H oxidase has been reported to produce superoxide ($O_2^{\bullet-}$) extracellularly as an autocrine/paracrine regulator or intracellularly as a signaling messenger in a variety of mammalian cells. However, it remains unknown how the activity of NAD(P)H oxidase is regulated in arterial myocytes. Recently, CD38-associated ADP-ribosylcyclase has been reported to use an NAD(P)H oxidase product, NAD^+ or $NADP^+$, to produce cyclic ADP-ribose (cADPR) or nicotinic acid adenine dinucleotide phosphate, which mediates intracellular Ca^{2+} signaling. This study was designed to test a hypothesis that the CD38/cADPR pathway as a downstream event exerts feedback regulatory action on the NAD(P)H oxidase activity in production of extra- or intracellular $O_2^{\bullet-}$ in mouse coronary arterial myocytes (CAMs). By fluorescence microscopic imaging, we simultaneously monitored extra- and intracellular $O_2^{\bullet-}$ production in wild-type ($CD38^{+/+}$) and CD38 knockout ($CD38^{-/-}$) CAMs in response to oxotremorine (OXO), a muscarinic type 1 receptor agonist. It was found that CD38 deficiency prevented OXO-induced intracellular but not extracellular $O_2^{\bullet-}$ production in CAMs. Consistently, the OXO-induced intracellular $O_2^{\bullet-}$ production was markedly inhibited by CD38 shRNA or the CD38 inhibitor nicotinamide in $CD38^{+/+}$ CAMs. Further, Nox4 siRNA inhibited OXO-induced intracellular but not extracellular $O_2^{\bullet-}$ production, whereas Nox1 siRNA attenuated both intracellular and extracellular $O_2^{\bullet-}$ production in $CD38^{+/+}$ CAMs. Direct delivery of exogenous cADPR into CAMs markedly elevated intracellular Ca^{2+} and $O_2^{\bullet-}$ production in $CD38^{-/-}$ CAMs. Functionally, CD38 deficiency or Nox1 siRNA and Nox4 siRNA prevented OXO-induced contraction in isolated perfused coronary arteries in CD38 WT mice. These results provide direct evidence that the CD38/cADPR pathway is an important controller of Nox4-mediated intracellular $O_2^{\bullet-}$ production and that CD38-dependent intracellular $O_2^{\bullet-}$ production is augmented in an autocrine manner by CD38-independent Nox1-derived extracellular $O_2^{\bullet-}$ production in CAMs.

There is a large body of evidence that NAD(P)H oxidase is a major source of $O_2^{\bullet-}$ in vascular cells [1–3] and that NAD(P)H oxidase is an important redox signaling enzyme for production of $O_2^{\bullet-}$ under physiological conditions to regulate vascular functions [4]. However, it remains poorly understood how the activity of vascular NAD(P)H oxidase is regulated in response to a variety of physiological and pathological stimuli. NAD(P)H oxidase and its isoforms have been reported to be expressed in cell membrane, cytosol, and various organelles, and it produces and releases $O_2^{\bullet-}$ in various cellular compartments [3,5–8]. Therefore, the temporospatial regulation of NAD(P)H oxidase activity is rather complicated. In this regard, recent studies have suggested that in the vasculature NAD(P)H oxidase and its isoforms can be detected in cell plasma membrane and various subcellular compartments, including the lamellipodial focal complexes, membrane ruffles, caveolae and lipid rafts, endosomes, sarcoplasmic reticulum, and nucleus [3,5–8]. This distribution of NAD(P)H oxidase may determine the concentrations of $O_2^{\bullet-}$ and related reactive oxygen species (ROS) within and outside vascular cells. In a recent study, we indeed demonstrated that in coronary arterial smooth muscle cells membrane-bound NAD(P)H oxidase produced $O_2^{\bullet-}$ toward the outside of these cells to regulate cell functions [9]. In other studies, NAD(P)H oxidase in cytosol and cell organelles such as lysosomes and sarcoplasmic reticulum contributed to intracellular levels of $O_2^{\bullet-}$ and ROS [3,10,11]. This intracellular $O_2^{\bullet-}$ and ROS may serve as second messengers to regulate cellular activities [12]. Upon various stimuli or agonists, NAD(P)H oxidase may be activated in different cellular compartments to produce $O_2^{\bullet-}$ thereby regulating cell function. How such compartmental production and action of $O_2^{\bullet-}$ are regulated remains a mystery.

Among the various regulatory pathways, CD38 is a multifunctional enzyme that uses NAD^+ or $NADP^+$ as substrate to produce related signaling molecules such as cyclic ADP-ribose (cADPR) and nicotinic acid adenine dinucleotide phosphate, the products of its ADP-ribosylcyclase activity that are potent intracellular Ca^{2+} mobilizers

* Corresponding author. Fax: +1 804 828 2117.
E-mail address: pli@vcu.edu (P.-L. Li).

0891-5849/$ – see front matter © 2011 Elsevier Inc. All rights reserved.
doi:10.1016/j.freeradbiomed.2011.10.485

[13]. Our recent studies have demonstrated that this CD38/ADP-ribosylcyclase-mediated signaling pathway contributes importantly to the vasomotor response. Because both NAD^+ and $NADP^+$, substrates for the ADP-ribosylcyclase of CD38, are the products of NAD(P)H oxidase, it is plausible that there may be an important interplay between CD38-mediated Ca^{2+} and NAD(P)H oxidase-mediated redox signaling. Such interplay of both signaling pathways was indeed found to be present in various cells or tissues. For example, it has been shown that production of ROS was markedly reduced in embryonic fibroblasts from $CD38^{-/-}$ mice, suggesting that ROS production may be dependent upon an intact CD38 signaling pathway [14]. On the other hand, $O_2^{\bullet-}$ and ROS were reported to promote CD38/ADP-ribosylcyclase activity to enhance Ca^{2+} signaling [15]. In this study, we attempted to test whether the CD38/ADP-ribosylcyclase signaling pathway participates in the regulation of NAD(P)H oxidase-dependent $O_2^{\bullet-}$ production extra- and intracellularly in coronary arterial myocytes (CAMs) in response to a muscarinic type 1 (M_1) agonist, a classical activator of CD38/ADP-ribosylcyclase in these cells [16]. We first examined whether intracellular $O_2^{\bullet-}$ production induced by the M_1 receptor agonist oxotremorine (OXO) is altered in CAMs from $CD38^{-/-}$ mice. Then, we tested the role of NAD(P)H oxidase in CD38-associated intracellular and extracellular $O_2^{\bullet-}$ production in CAMs. We further determined whether induction of intracellular Ca^{2+} release by exogenous supplementation with cADPR could restore intracellular $O_2^{\bullet-}$ production in $CD38^{-/-}$ CAMs. Finally, we examined the role of CD38/cADPR-associated $O_2^{\bullet-}$ production in the vasoconstrictor action of OXO in coronary arteries.

Materials and methods

Mice

Both $CD38^{-/-}$ and wild-type mice were purchased from The Jackson Laboratory. Male and female mice, 8 weeks of age, were used in all experiments. All experimental protocols were reviewed and approved by the Animal Care Committee of Virginia Commonwealth University.

Isolation and culture of mouse CAMs

CAMs were isolated from $CD38^{+/+}$ or $CD38^{-/-}$ mice as previously described [17]. In brief, mice were deeply anesthetized with intraperitoneal injection of pentobarbital sodium (25 mg/kg). The heart was excised with an intact aortic arch and immersed in a petri dish filled with ice-cold Krebs–Henseleit solution (20 mM Hepes, 128 mM NaCl, 2.5 mM KCl, 2.7 mM $CaCl_2$, 1 mM $MgCl_2$, 16 mM glucose, pH 7.4). A 25-gauge needle filled with Hanks' buffered saline solution (HBSS; 5.0 mM KCl, 0.3 mM KH_2PO_4, 138 mM NaCl, 4.0 mM $NaHCO_3$, 0.3 mM $Na_2HPO_4 \cdot 7H_2O$, 5.6 mM D-glucose, and 10.0 mM Hepes, with 2% antibiotics) was inserted into the aortic lumen opening while the whole heart remained in the ice-cold buffer solution. The opening of the needle was inserted deep into the heart close to the aortic valve. The needle was tied in place with the needle tip as close to the base of the heart as possible. The infusion pump was started with a 20-ml syringe containing warm HBSS through an intravenous extension set at a rate of 0.1 ml/min for 15 min. HBSS was replaced with warm enzyme solution (1 mg/ml collagenase type I, 0.5 mg/ml soybean trypsin inhibitor, 3% bovine serum albumin (BSA), and 2% antibiotic–antimycotic), which was flushed through the heart at a rate of 0.1 ml/min. Perfusion fluid was collected at 30-, 60-, and 90-min intervals. At 90 min, the heart was cut with scissors, and the apex was opened to flush out the cells that collected inside the ventricle. The fluid was centrifuged at 1000 rpm for 10 min, the cell-rich pellets were mixed with the one of the media described below, and the cells were plated on 2% gelatin-coated six-well plates and incubated in 5% CO_2–95% O_2 at 37 °C. Advanced Dulbecco's modified Eagle's medium (DMEM) with 10% fetal bovine serum, 10% mouse serum, and 2% antibiotics was used for isolated smooth muscle cells. The medium was replaced 3 days after cell isolation and then once or twice each week until the cells grew to confluence. Mouse CAMs were identified according to their morphology, immunohistological staining, Western blot analysis of marker proteins, and flow-cytometric characteristics (Fig. 1). In these experiments, smooth muscle α-actin (α-SMA) and Dil-Ac-LDL (Biomedical Technology) were used as markers of smooth muscle cells and vascular endothelial cells.

Simultaneous monitoring of $O_2^{\bullet-}$ production inside and outside CAMs

Intracellular and extracellular $O_2^{\bullet-}$ production was simultaneously monitored by fluorescence microscopy as we previously described [9]. $O_2^{\bullet-}$ oxidizes dihydroethidium (DHE) to form membrane-impermeative ethidium, which binds to DNA and forms a strong red fluorescence. In this regard, intracellular $O_2^{\bullet-}$ production is detected when $O_2^{\bullet-}$ oxidizes intracellular DHE to ethidium, which binds to nuclear DNA, whereas extracellular $O_2^{\bullet-}$ oxidizes DHE in the solution to ethidium, which binds to Matrigel (BD Biosciences)-trapped extracellular DNA. In these experiments, freshly isolated CAMs (10^2 cells/well) were seeded into a 16-well chamber slide with a transparent glass bottom (Lab-Tek) and incubated overnight. On the day of the experiment, the CAMs were washed twice with Hanks' buffer, and 40 μl of salmon testes DNA solution (7.5 mg/ml; Sigma, St. Louis, MO, USA) was mixed with 40 μl of Matrigel solution (at 4 °C) and then carefully loaded onto the top of the CAMs. After 5 min at room temperature, the gel was polymerized and exogenous DNA was immobilized around these cells. The CAMs with Matrigel were then overlaid with Hanks' buffer containing 250 μM DHE. After 60 min loading of DHE into the CAMs, the chamber slide was mounted on the stage of a fluorescence microscope, which we routinely used for high-speed wavelength-switching imaging acquisition and recording. For both intracellular and extracellular DHE oxidizing signals, the ratio of ethidium–DNA to DHE signal was recorded at an excitation of 480 nm and an emission of 610 nm. The DHE fluorescence signal was detected at an excitation of 380 nm and an emission of 445 nm. The ratio of ethidium–DNA to DHE fluorescent signal was recorded to represent $O_2^{\bullet-}$ levels. The ratiometric assay increases the sensitivity for $O_2^{\bullet-}$ detection and avoids an artifact in assays from cell volume changes or contractions during agonist stimulation. For each experiment, 8–10 CAMs were monitored simultaneously and an average value was used for statistical analysis. OXO (80 μM) was added to activate its receptor and consequently stimulate $O_2^{\bullet-}$ production. Nicotinamide (6 mM) was preincubated with the cells for 30 min, or CD38 short-hairpin RNA (shRNA) was transferred into wild-type CAMs, and then the $O_2^{\bullet-}$-production response to OXO was determined.

Confocal microscopic detection of extracellular $O_2^{\bullet-}$ production

To further determine extracellular $O_2^{\bullet-}$, CAMs were prepared as described above for ethidium–DNA trapping imaging [9]. In brief, 0.5 ml of Matrigel was mixed with 25 μl of OxyBURST H_2HFF green BSA (10 μg/ml), a BSA-conjugated molecular probe that directly reacts with H_2O_2, and then used to evenly coat the 35×10-mm cell culture dish. A freshly isolated CAM suspension (60 μl, 3×10^6/ml) was loaded on the top of the ice-cold Matrigel matrix, and then the culture dish was gently tapped three or four times to distribute cells across the surface of the gel. After the gel polymerized at room temperature for 5 min, 2 ml of Krebs–Ringer phosphate buffer, which contains PBS, pH 7.4, with 1.0 mM Ca^{2+}, 1.5 mM Mg^{2+}, and 5.5 mM glucose, was added. Confocal fluorescence microscopy images were acquired by an Olympus Fluoview system (version 4.2, FV300), consisting of an Olympus BX61WI inverted microscope with an Olympus Lumplan

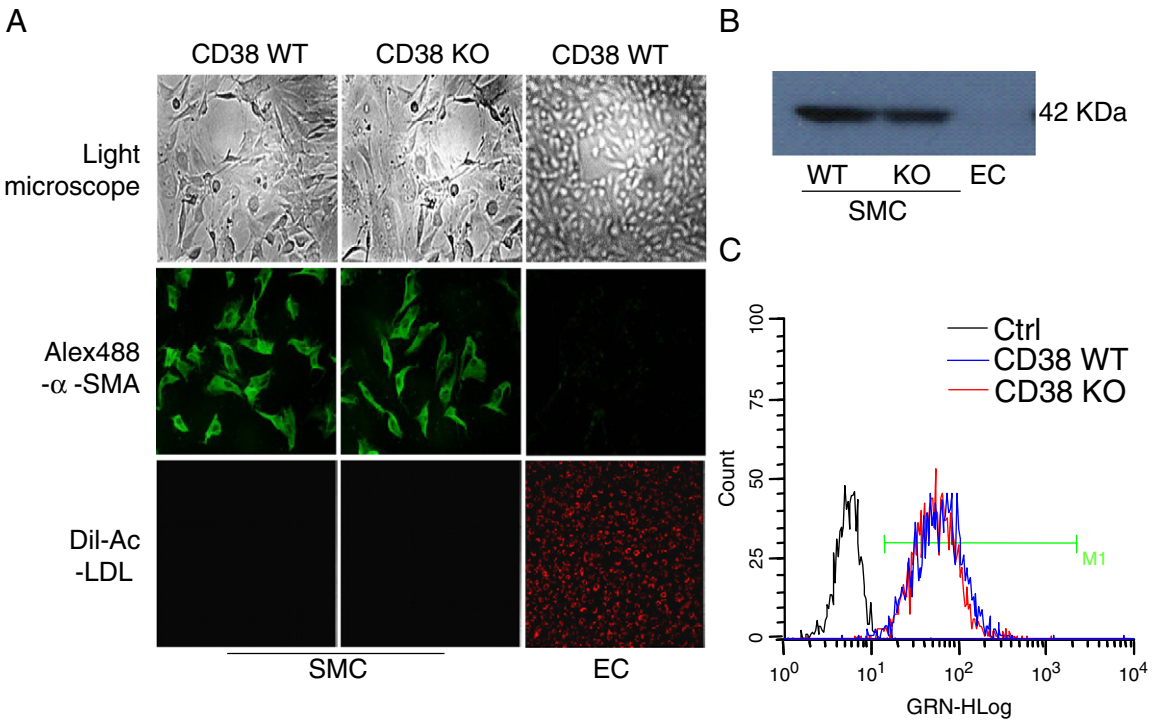

Fig. 1. Coronary artery smooth muscle cell characterization. (A) The top shows cell morphology of CD38 WT and KO CAMs and CAECs under light microscopy. The middle shows immunocytochemistry of CAMs and CAECs that were stained first with an α-SMA antibody followed by an Alexa-488-conjugated second antibody. The bottom shows that Dil-Ac-LDL labels CAMs and CAECs. (B) Western blot assay for α-SMA protein expression in CAMs and CAECs. (C) Flow cytometry assay for the purity of CAMs, which were stained with α-SMA antibodies followed by Alexa-488-conjugated second antibody. Black peak represents control for CD38 WT and KO CAMs without staining with α-SMA first antibody. Blue and red peaks represent positive stain for α-SMA of CD38 WT and KO CAMs. M1, cutoff point for estimating percentage of positive stain.

F1 × 60, 0.9 numerical aperture, water-immersion objective. A single *Z* section was taken or 0.1-μm sections were obtained through the cell with excitation and emission wavelengths of 488 and 530 nm, respectively, for OxyBURST. Real-time microscopic fluorescence images were acquired every 1 or 2 min under control conditions and after different treatments. This OxyBURST H_2HFF green BSA detects H_2O_2, which mirrors $O_2^{\bullet-}$ production outside the cells because BSA cannot enter the cells [18].

Electronic spin resonance (ESR) detection of extracellular and intracellular $O_2^{\bullet-}$ level

For the detection of the total and extracellular $O_2^{\bullet-}$ production dependent on NAD(P)H oxidase, the proteins from CAMs extracted using sucrose buffer or from gently collected cells were resuspended with modified Krebs–Hepes buffer containing deferoximine (100 μmol/L; Sigma) and diethyldithiocarbamate (5 μmol/L; Sigma). Intact cells (1×10^6) or their homogenates were subsequently mixed with 1 mM cell-permeative $O_2^{\bullet-}$-specific spin trap, 1-hydroxy-3-methoxycarbonyl-2,2,5,5-tetramethylpyrrolidine, and substrate NAD(P)H in the presence or absence of manganese-dependent superoxide dismutase (SOD; 200 U/ml; Sigma). The mixture was loaded into glass capillaries and immediately analyzed for $O_2^{\bullet-}$ production kinetically for 10 min using a Miniscope MS200 ESR spectrometer (Magnettech Ltd., Berlin, Germany) as we described earlier [19]. The SOD-inhibitable fraction of the signal in intact cells or homogenates reflects the extracellular or total $O_2^{\bullet-}$ level, respectively. The difference between the total and the extracellular $O_2^{\bullet-}$ level was used to reflect intracellular $O_2^{\bullet-}$ level. The ESR settings were as follows: biofield, 3350; field sweep, 60 G; microwave frequency, 9.78 GHz; microwave power, 20 mW; modulation amplitude, 3 G; 4096 points of resolution; receiver gain, 20 for tissue and 50 for cells [20]. The results were expressed as fold changes relative to control.

Fluorescence measurement of $[Ca^{2+}]_i$ and cADPR delivery in CAMs

Intracellular Ca^{2+} responses to OXO or cADPR were determined using a fluorescence image analysis system with the Ca^{2+} indicator fura-2, as described previously [15,21]. Ca^{2+}-free HBSS including 1 mM EGTA was used for Ca^{2+} measurement to ensure the Ca^{2+} response was solely derived from intracellular Ca^{2+} store release rather than from extracellular Ca^{2+} influx. Administration of cADPR (200 μM) to the cells was carried out by wrapping this cell-impermeative nucleotide in Optison (Perflutren protein-type A microspheres) and delivering it by ultrasound treatment as detailed previously [22–24].

Isolated small artery for tension recording

Small ventricular septal arteries (~150-μm inner diameter) were dissected [25] and then mounted in a Multi Myograph 610 M (Danish Myo Technology, Aarhus, Denmark) for recording of isometric wall tension [26,27] after 30 min of equilibration in physiological salt solution (PSS; pH 7.4) containing (in mM) 119 NaCl, 4.7 KCl, 1.6 $CaCl_2$, 1.17 $MgSO_4$, 1.18 NaH_2PO_4, 2.24 $NaHCO_3$, 0.026 EDTA, and 5.5 glucose at 37 °C bubbled with a gas mixture of 95% O_2 and 5% CO_2. After the basic tension was set, the dose effects of OXO alone (0, 20, 40, 60, 80, and 100 μM) on the tension changes in wild-type and $CD38^{-/-}$ septal arterial wall were measured with or without the presence of various inhibitors, including 8-Br-cADPR (30 μM) or Nox1 and Nox4 short interfering RNA (siRNA). Ultrasound microbubble technology was used to transfect mouse coronary artery smooth muscle with Nox1 and Nox4 siRNA as we described previously [22,23,28,29]. In brief, after isolation, coronary arteries were transferred to a water-jacketed perfusion chamber and cannulated with two glass micropipettes at their in situ length, with PSS buffer in the lumen until transfection. SiRNA (20 μg) was mixed in 100 μl Optison (Amersham) and kept for 30 s at 37 °C. Then the RNA–Optison solution was perfused within the lumen of arteries. The arteries were treated with ultrasound

for 1 min through a 6-mm-diameter probe in the chamber with an input frequency of 1 MHz, an output intensity of 1.0–2.0 W/cm^2, and a pulse duty ratio of 10–50% (Rich-Mar). After transfection, the arteries were removed from the glass micropipettes and incubated in DMEM for 24–48 h at 37 °C to knock down Nox1 and Nox4.

Statistics

Data are presented as means ± SE. Significant differences between and within multiple groups were examined using ANOVA for repeated measures, followed by Duncan's multiple-range test. The Student *t* test was used to detect significant differences between two groups. $P<0.05$ was considered statistically significant.

Results

Coronary artery smooth muscle cell characterization

As shown on the top of Fig. 1A, CAMs formed longitudinal bands of parallel cells and became thinner at a high density. Immunocytochemistry (Fig. 1A, middle) showed that CD38 WT and KO CAMs were stained positively with anti-α-SMA antibody followed by Alexa-488-conjugated second antibody. However, no staining was found in coronary arterial endothelial cells (CAECs). Similarly, Western blot analysis showed that α-SMA was detected only from CD38 WT and KO CAMs and not endothelial cells (Fig. 1B). Moreover, Dil-Ac-LDL, vascular endothelial cell marker, labeled only endothelial cells to produce red fluorescence (Fig. 1A, bottom). To further ascertain the purity of CAMs, the percentage of α-SMA-positive CAMs was assessed with flow cytometry. The results showed that the purity was 97.6% for α-SMA-stained CD38 WT CAMs and 98.0% for CD38 KO CAMs (Fig. 1C).

Lack of intracellular, but not extracellular, $O_2^{\bullet-}$ production in CAMs from CD38$^{-/-}$ mice

To determine whether CD38 has a role in agonist-induced $O_2^{\bullet-}$ production in CAMs, we simultaneously monitored the fluorescence intensity of the ethidium–DNA complex within CD38$^{+/+}$ and CD38$^{-/-}$ CAMs and in Matrigel around these cells. Fig. 2A shows representative fluorescence images before and 50 min after a CAM received OXO at a concentration of 80 μM. The dynamic changes in ratio of intracellular and extracellular ethidium–DNA fluorescent signal to DHE fluorescent signal were acquired and are summarized in Fig. 2B. We found that OXO induced increases in extracellular $O_2^{\bullet-}$ levels (becoming red) in both CD38$^{+/+}$ and CD38$^{-/-}$ CAMs (Fig. 2A). In addition, CD38 deficiency has no effect on the dynamic responses of extracellular ethidium–DNA fluorescence in CAMs (Fig. 2B). In contrast, OXO-induced increases in $O_2^{\bullet-}$ levels inside cells were markedly attenuated in CD38$^{-/-}$ CAMs compared to those in CD38$^{+/+}$ CAMs. Therefore, our findings suggest that CD38 is key for agonist-induced intracellular $O_2^{\bullet-}$ production in CAMs.

We also examined whether OXO induces similar extracellular ROS production between CD38$^{+/+}$ and CD38$^{-/-}$ CAMs using OxyBURST green, which is a BSA-conjugated probe and directly reacts with H_2O_2. Because $O_2^{\bullet-}$ rapidly dismutates into H_2O_2, OxyBURST green fluorescence intensity in extracellular Matrigel reflects extracellular $O_2^{\bullet-}$-derived ROS levels. Fig. 3A shows representative confocal fluorescence images from CAMs. OXO stimulation induced similar increases in OxyBURST green fluorescence in CD38$^{+/+}$ and CD38$^{-/-}$ CAMs. As summarized in Fig. 3B, CD38 deficiency has no effect on OXO-induced dynamic responses of OxyBURST green fluorescence in CAMs.

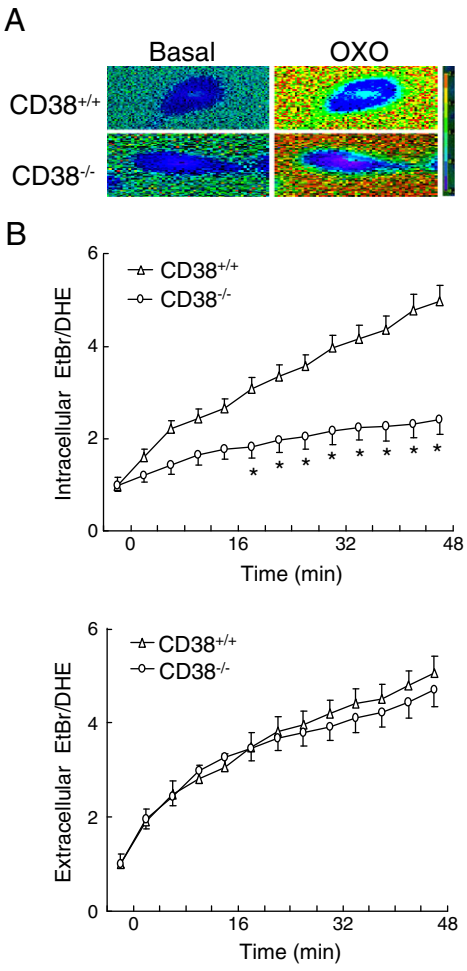

Fig. 2. Fluorescence microscopic imaging analysis to simultaneously monitor the OXO-induced $O_2^{\bullet-}$ production inside and outside single coronary arterial myocytes from CD38$^{+/+}$ and CD38$^{-/-}$ mice. (A) Typical time-dependent increase in oxidized DHE fluorescence ratio (ethidium bromide (EtBr)/DHE) image inside and outside a CAM. Red fluorescence indicates $O_2^{\bullet-}$ level higher than blue background. (B) Summarized digitized data showing the spatiotemporal pattern of $O_2^{\bullet-}$ increase inside and outside CD38$^{+/+}$ and CD38$^{-/-}$ CAM during OXO (80 μM) stimulation ($n=6$, $^*P<0.05$ vs CD38$^{+/+}$ CAM).

Inhibition of CD38/cADPR signaling pathway blocked intracellular $O_2^{\bullet-}$ production without effect on extracellular $O_2^{\bullet-}$ production in CAMs from CD38$^{+/+}$ mice

CD38 is a key enzyme for production and metabolism of cADPR in vascular cells. We then examined whether CD38/cADPR is involved in OXO-induced intracellular $O_2^{\bullet-}$ production. As shown in Fig. 4, inhibiting CD38-mediated cADPR production with nicotinamide, or knockdown of CD38 via RNA interference, inhibited OXO-induced increases in intracellular but not extracellular $O_2^{\bullet-}$ production in CAMs.

By using the ESR spectrometry, we further determined the role of CD38/cADPR in OXO-induced intracellular $O_2^{\bullet-}$ production in CAMs. Fig. 5A shows representative changes in SOD-inhibitable ESR spectrometric curve recorded under control conditions and after OXO stimulation. Summarized data show that OXO significantly increased production of $O_2^{\bullet-}$ dependent on NAD(P)H oxidase outside and inside CD38$^{+/+}$ CAMs. Inhibition of CD38/cADPR by CD38 inhibitor nicotinamide or cADPR antagonist 8-Br-cADRP attenuated OXO-induced SOD-sensitive $O_2^{\bullet-}$ production inside but not outside CD38$^{+/+}$ CAMs. Similarly, knockdown of CD38 by CD38 shRNA or genetic deficiency of CD38 inhibited intracellular but not extracellular SOD-sensitive $O_2^{\bullet-}$ production in CAMs (Fig. 5B).

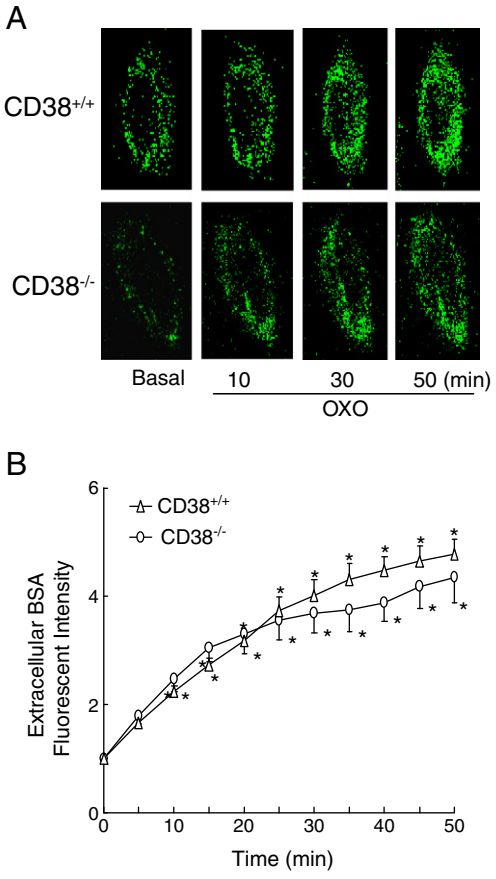

Fig. 3. Confocal microscopic analysis to monitor $O_2^{\bullet-}$ outside of CAMs from $CD38^{+/+}$ and $CD38^{-/-}$ mice. (A) Representative images showing extracellular $O_2^{\bullet-}$ production as detected by OxyBURST H2HFF green BSA-trapped H_2O_2 outside a single CAM during OXO (80 μM) stimulation. (B) Summarized digitized data showing the time-dependent $O_2^{\bullet-}$ increases outside $CD38^{+/+}$ and $CD38^{-/-}$ CAMs ($n=6$, $^*P<0.05$ vs basal condition).

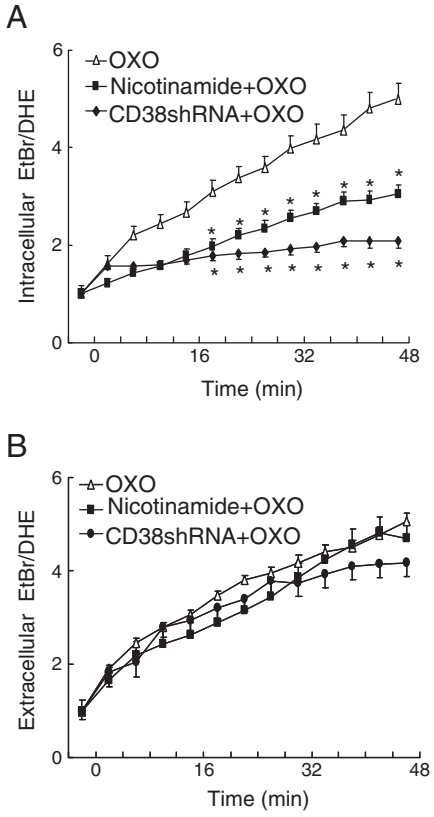

Fig. 4. Effect of CD38 gene silencing or inhibition of ADP-ribosylcyclase activity of CD38 on OXO-induced (A) intracellular and (B) extracellular $O_2^{\bullet-}$ production in $CD38^{+/+}$ CAMs. The CD38 gene was silenced by CD38 shRNA and CD38 cyclase activity was inhibited by nicotinamide. $CD38^{+/+}$ CAM was treated with OXO (80 μM) for 50 min in the presence or absence of CD38 shRNA or nicotinamide ($n=6$, $^*P<0.05$ vs OXO-treated CAM).

Regulation of NAD(P)H oxidase isoform activity by CD38–cADPR-mediated signaling in CAMs

We previously reported that Nox4 mediates only intracellular $O_2^{\bullet-}$ production, whereas Nox1 is involved in both extracellular and intracellular $O_2^{\bullet-}$ production in bovine CAMs [9]. To further examine the mechanism of CD38-associated intracellular $O_2^{\bullet-}$ production, we determined ethidium/DHE fluorescence in mouse CAMs transfected with Nox4 siRNA or Nox1 siRNA. Nox1 and Nox4 siRNA have been demonstrated to inhibit the protein expression of Nox1 and Nox4 by 66.5 and 77.4%, respectively (Fig. 6). It was found that Nox4 siRNA or Nox1 siRNA significantly inhibited intracellular $O_2^{\bullet-}$ production in $CD38^{+/+}$ CAMs (Fig. 7A), whereas intracellular $O_2^{\bullet-}$ production was not further decreased by Nox4 siRNA or Nox1 siRNA in $CD38^{-/-}$ CAMs (Fig. 7C). Moreover, Nox1 siRNA but not Nox4 siRNA blocked extracellular $O_2^{\bullet-}$ production in both $CD38^{+/+}$ and $CD38^{-/-}$ CAMs (Figs. 7B and D).

Exogenous cADPR restored intracellular $O_2^{\bullet-}$ production without effect on extracellular $O_2^{\bullet-}$ production in $CD38^{-/-}$ CAMs

To confirm that failure of cADPR/Ca^{2+} response during OXO stimulation contributes to the defect in intracellular $O_2^{\bullet-}$ production in $CD38^{-/-}$ CAMs, we determined whether exogenous supplementation of cADPR restores Ca^{2+} response and $O_2^{\bullet-}$ production. As shown in Figs. 8A and B, exogenous cADPR triggered similar increases in intracellular Ca^{2+} concentration in $CD38^{+/+}$ (from 184 to 321 nM) and $CD38^{-/-}$ CAMs (from 175 to 325 nM). Moreover, exogenous cADPR

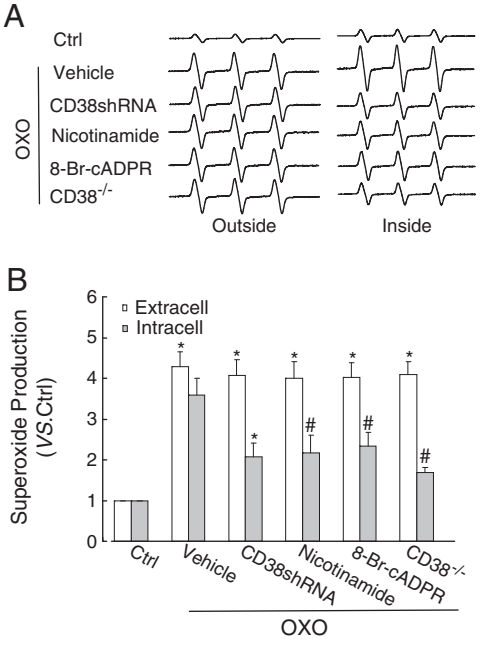

Fig. 5. ESR spectrometric analysis of $O_2^{\bullet-}$ production in CAMs stimulated by OXO. (A) Representative ESR spectrographs of $O_2^{\bullet-}$ trapped by 1-hydroxy-3-methoxycarbonyl-2,2,5,5-tetramethylpyrrolidine. (B) Summarized data showing the effects of CD38 shRNA, nicotinamide (6 mM), 8-Br-cADPR (30 μM), or CD38 deficiency on OXO-induced $O_2^{\bullet-}$ production inside or outside $CD38^{+/+}$ CAMs ($n=6$, $^*P<0.05$ vs unstimulated samples (control); $^{\#}P<0.05$ vs samples treated with OXO alone).

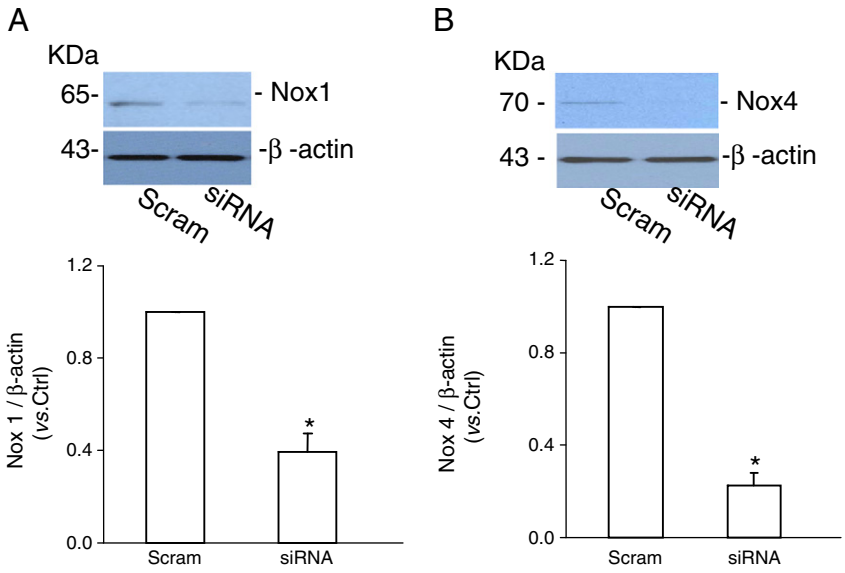

Fig. 6. Western blot gel document presents the levels of (A) Nox1, (B) Nox4, and β-actin from mouse CAMs before and after Nox1 and Nox4 siRNA. Summarized results show normalized intensity ratio of Nox1 and Nox4 to β-actin. Nox1 and Nox4 protein expression was significantly inhibited when Nox1 and Nox4 siRNA was transfected into mouse CAMs ($n=3$, $^*P<0.05$ vs scramble-RNA-transfected CAMs).

induced similar intracellular but not extracellular $O_2^{\bullet-}$ production in CD38$^{+/+}$ and CD38$^{-/-}$ CAMs.

Vasoconstrictor response of coronary arteries to M_1 receptor activation in CD38$^{+/+}$ and CD38$^{-/-}$ mice

To examine the functional relevance of CD38/cADPR signaling-mediated regulation of $O_2^{\bullet-}$ production, we examined the vasoconstrictor response of isolated perfused coronary arteries from both CD38$^{+/+}$ and CD38$^{-/-}$ mice to OXO, a typical M_1 receptor agonist. As shown in Fig. 9A, OXO dose-dependently induced vasoconstriction in coronary arteries from CD38$^{+/+}$ mice with a maximum response of 56.9 ± 12.4% at the dose of 100 μM. This OXO-induced vasoconstriction response was significantly reduced in CD38$^{-/-}$ arteries with a maximum response of 14.5 ± 2.9%. Blockade of cADPR signaling using the cADPR antagonist 8-Br-cADPR or inhibition of Nox1 or Nox4 by its siRNA significantly attenuated OXO-induced vasoconstriction in CD38$^{+/+}$ arteries (Fig. 9B). Moreover, Nox1 or Nox4 siRNA had no effect on OXO-induced residual vasoconstrictor response in CD38$^{-/-}$ arteries (Fig. 9C).

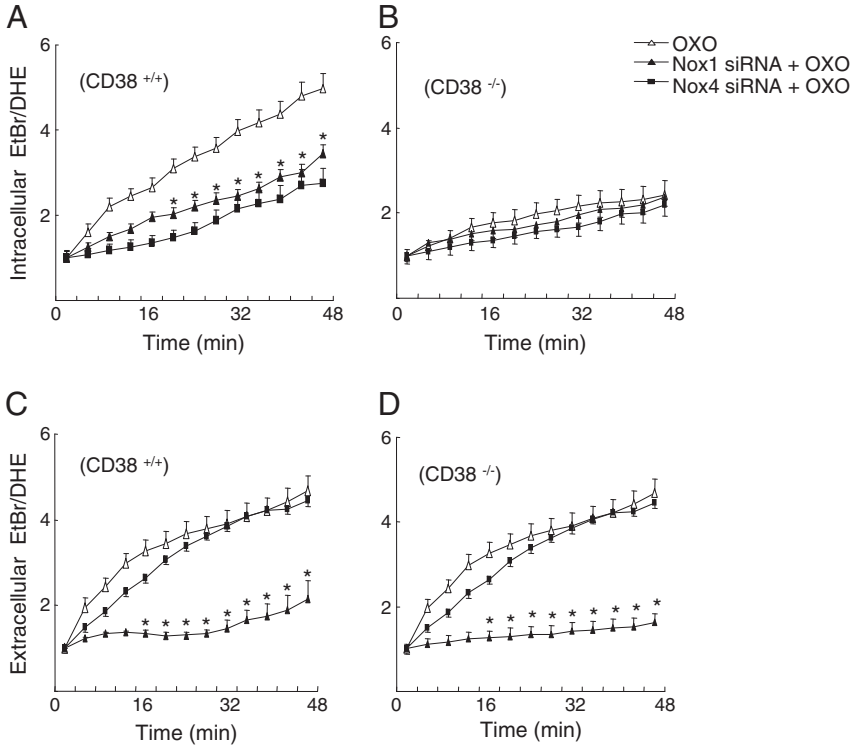

Fig. 7. Effects of NAD(P)H oxidase inhibition on OXO-induced $O_2^{\bullet-}$ production. (A, B) Transfected Nox1 and Nox4 siRNA suppressed $O_2^{\bullet-}$ production inside CD38$^{+/+}$ CAM; however, Nox1 and Nox4 siRNA had no significant effects on $O_2^{\bullet-}$ production inside CD38$^{-/-}$ CAM. (C, D) $O_2^{\bullet-}$ production outside CD38$^{+/+}$ and CD38$^{-/-}$ cells was inhibited by pretreatment with Nox1 siRNA, whereas extracellular $O_2^{\bullet-}$ production was not affected by Nox4 siRNA ($n=6$, $^*P<0.05$ vs CAM treated with OXO alone).

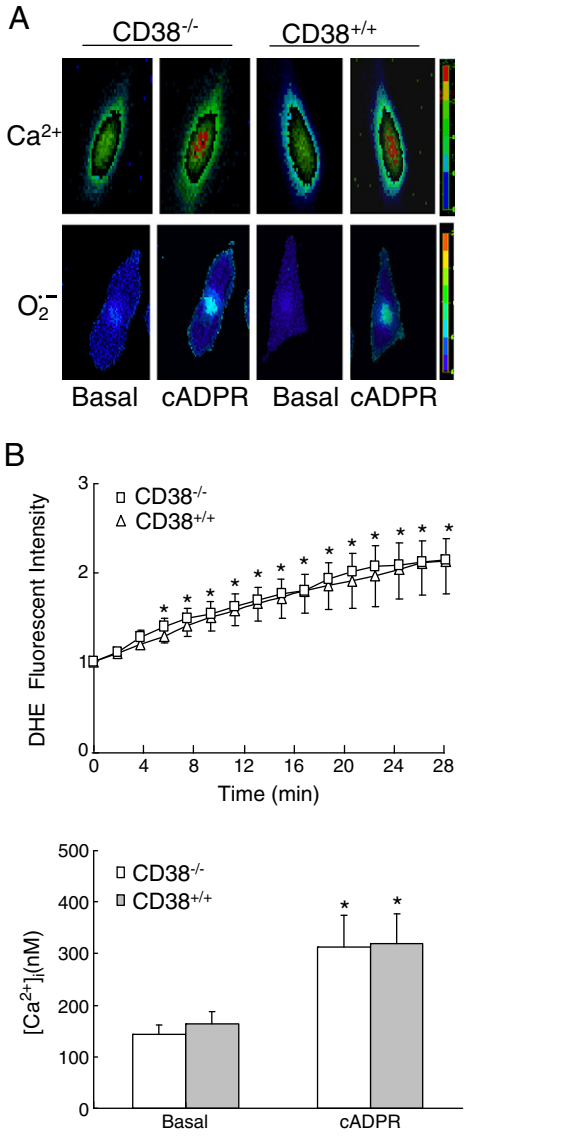

Fig. 8. Effects of exogenous cADPR on Ca^{2+} release and $O_2^{\bullet-}$ production in CAMs. (A) Typical fluorescence images of $CD38^{+/+}$ and $CD38^{-/-}$ CAMs stained by DHE or fura-2 before (basal) and after cADPR (200 μM) introduction. (B, C) Summarized data showing exogenous cADPR-induced increases in intracellular $O_2^{\bullet-}$ and Ca^{2+} concentration inside $CD38^{+/+}$ and $CD38^{-/-}$ CAMs ($n=6$, $^*P<0.05$ compared with basal levels).

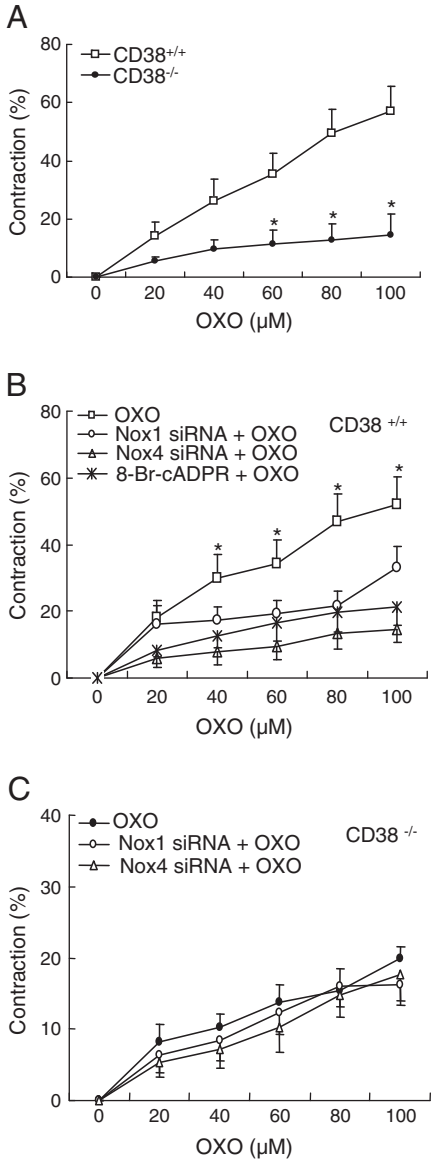

Fig. 9. Effects of (A) CD38 deficiency and (B, C) NAD(P)H oxidase inhibition or cADPR/Ca^{2+} blockade on OXO-induced vasoconstriction in coronary arteries. cADPR antagonist, 8-Br-cADPR (30 μM), or Nox1 and Nox4 siRNA was used ($n=3$, $^*P<0.05$ compared with $CD38^{+/+}$ artery).

Discussion

This study has demonstrated that the CD38/cADPR pathway is involved in OXO-induced intracellular but not extracellular $O_2^{\bullet-}$ production in CAMs. CD38-regulated intracellular $O_2^{\bullet-}$ production is dependent on intracellular cADPR/Ca^{2+} signaling and NAD(P)H oxidase activity. Further, this CD38-mediated signaling can be augmented by membrane-bound NAD(P)H oxidase-derived extracellular $O_2^{\bullet-}$. These findings reveal that extracellular $O_2^{\bullet-}$ enhances CD38/cADPR-regulated intracellular $O_2^{\bullet-}$ production in CAMs upon M_1 receptor activation.

Using fluorescence imaging with several ROS measurement methods, we first compared the spatiotemporal pattern of $O_2^{\bullet-}$ production in $CD38^{+/+}$ and $CD38^{-/-}$ CAMs by using a sensitive and dynamic measurement of $O_2^{\bullet-}$ production both inside and outside cells. This method was developed in our laboratory by modifying a high-speed wavelength-switching fluorescence microscopic imaging system that we used for simultaneous monitoring of Ca^{2+} and nitric oxide [30]. With the help of Matrigel to trap DNA around CAMs, we were able to simultaneously measure extracellular and intracellular DHE-oxidizing signals, which represent $O_2^{\bullet-}$ levels. In this study, we used this assay and found that the OXO-induced M_1-receptor activation stimulated $O_2^{\bullet-}$ production both outside and inside $CD38^{+/+}$ CAMs with a spatiotemporal pattern in which more rapid extracellular increase in $O_2^{\bullet-}$ levels was followed by a slow increase in intracellular $O_2^{\bullet-}$ levels, which was similar to those previously observed in bovine CAMs [9]. More importantly, this study showed that OXO-induced increases in intracellular $O_2^{\bullet-}$ levels were abolished in $CD38^{-/-}$ CAMs or in $CD38^{+/+}$ CAMs transfected with CD38 shRNA. In contrast, no difference in OXO-induced extracellular $O_2^{\bullet-}$ productions was found between $CD38^{+/+}$ and $CD38^{-/-}$ CAMs. These findings indicate that CD38 is essentially involved in OXO-induced intracellular $O_2^{\bullet-}$ production in CAMs. Consistent with our findings, a recent study in mouse embryonic fibroblasts has shown that production of ROS in $CD38^{-/-}$ cells was markedly reduced compared with $CD38^{+/+}$ cells during hypoxia/reoxygenation [14]. Based on these observations, we believe that M_1-receptor activation results in at least two distinct pathways for $O_2^{\bullet-}$ production in CAMs, namely,

CD38-dependent intracellular $O_2^{\bullet-}$ production and CD38-independent extracellular $O_2^{\bullet-}$ production.

To further determine the contribution of the CD38/cADPR pathway to intracellular $O_2^{\bullet-}$ production, we examined whether OXO-induced intracellular $O_2^{\bullet-}$ increases can be blocked in wild-type CAMs by two widely used cADPR signaling inhibitors—nicotinamide (an inhibitor of ADP-ribosylcyclase activity of CD38, which is responsible for synthesis of cADPR) and 8-Br-cADPR (a cADPR antagonist). Fluorescence imaging analysis and ESR studies demonstrated that, in the presence of nicotinamide, OXO-induced $O_2^{\bullet-}$ production inside $CD38^{+/+}$ CAMs was significantly reduced. In addition, blockade of the cADPR pathway by 8-Br-cADPR inhibited OXO-induced intracellular $O_2^{\bullet-}$ production as detected by ESR. These findings support the view that intracellular $O_2^{\bullet-}$ is associated with increases in ADP-ribosylcyclase activity of CD38 and synthesis of cADPR in wild-type CAMs during M_1-receptor activation.

NAD(P)H oxidase has been reported to be a major source of ROS in the vasculature [2]. The vascular NAD(P)H oxidase has characteristics of phagocyte NAD(P)H oxidase, which is composed of two transmembrane-bound catalytic proteins of $gp91^{phox}$ and $p22^{phox}$ and three cytosolic subunits of $p47^{phox}$, $p67^{phox}$, and $p40^{phox}$. In addition to $gp91^{phox}$, named as Nox2, some other homologues of $gp91^{phox}$ such as Nox1, Nox4, and Nox5 were identified in vascular cells such as endothelial and smooth muscle cells [1]. It has been shown that Nox2 localizes in plasma membranes as well as in intracellular compartments, and activation of Nox2 causes $O_2^{\bullet-}$ production in response to a variety of agonists such as angiotensin II in vascular cells [9]. In addition to Nox2, recent studies have indicated that Nox4 is primarily responsible for intracellular $O_2^{\bullet-}$ production localized in various organelles of vascular smooth muscle cells including the sarcoplasmic reticulum (SR), whereas Nox1 mainly produces extracellular $O_2^{\bullet-}$ [3,9,31]. In this regard, Nox1 has been shown to be enriched in the membrane fraction and Nox4 is predominately found in the intracellular compartments such as the SR of vascular cells [3,5]. In the present study, the use of Nox4 siRNA to silence this gene significantly attenuated OXO-induced intracellular $O_2^{\bullet-}$ production in $CD38^{+/+}$ CAMs, but it did not have further effects in $CD38^{-/-}$ CAMs. These results suggest that CD38/cADPR-regulated intracellular $O_2^{\bullet-}$ production is primarily dependent on Nox4 activity inside CAMs. However, introduction of siRNA to silence the Nox1 gene significantly attenuated not only OXO-induced intracellular $O_2^{\bullet-}$ production, but also extracellular $O_2^{\bullet-}$ in $CD38^{+/+}$CAMs, suggesting that Nox1 may contribute to the production of both intra- and extracellular $O_2^{\bullet-}$. It has been well documented that the production of cADPR is increased by oxidants, which is dependent on the redox regulation of ADP-ribosylcyclase activity of CD38 possibly via enzyme dimerization causing enhancement of its activity [15,32,33]. As we demonstrated in our previous study, extracellular $O_2^{\bullet-}$ serves as an autocrine to enhance CD38-dependent intracellular $O_2^{\bullet-}$ production in response to M_1 receptor activation. This action of Nox1-dependent extracellular $O_2^{\bullet-}$ production may be associated with redox activation of ADP-ribosylcyclase activity of CD38.

Another important finding of this study was that delivery of exogenous cADPR into cells resulted in intracellular Ca^{2+} release and restored intracellular $O_2^{\bullet-}$ production in $CD38^{-/-}$ CAMs. This finding provides direct evidence that cADPR-induced intracellular Ca^{2+} mobilization is coupled with activation of intracellular NAD(P)H oxidase in CAMs. Previous studies have shown that Nox4 activity is sensitive to intracellular Ca^{2+} regulation associated with cADPR-induced Ca^{2+} release from the ryanodine receptor, a Ca^{2+} channel on the SR membrane [3,10,34]. In this study, Nox4 was also demonstrated to primarily contribute to OXO-induced intracellular $O_2^{\bullet-}$ production. Therefore, it is possible that CD38-derived cADPR production induces Ca^{2+} mobilization from the SR and thereby results in local activation of Nox4 on the SR. Indeed, silencing the Nox4 gene was also found to substantially attenuate intracellular $O_2^{\bullet-}$ production induced by direct delivery of cADPR into the CAMs from wild-type mice. Moreover, exogenous cADPR did not increase extracellular $O_2^{\bullet-}$ levels in these CAMs, indicating that cADPR–Ca^{2+} signaling does not participate in the activation of Nox1 or Nox2 and consequent extracellular $O_2^{\bullet-}$ production in CAMs. This further confirms the findings obtained from CAMs with CD38 deficiency or blockade of cADPR signaling that OXO-induced extracellular $O_2^{\bullet-}$ production remains to occur. Thus, it is possible that Nox1 activation is an upstream event of cADPR signaling, but the Nox4 activation is a downstream event of cADPR signaling in CAMs. However, a recent study has shown that Nox1 mRNA level was markedly lower in cultured mouse embryonic fibroblasts from $CD38^{-/-}$ mice compared to wild-type cells during hypoxia/reoxygenation and that the transcription of Nox1 mRNA was up-regulated by the calcium ionophore ionomycin in these wild-type cells [14]. It seems that CD38/cADPR–Ca^{2+} signaling also controls Nox1-derived extracellular $O_2^{\bullet-}$ production in mouse embryonic fibroblasts by alteration of Nox1 expression. Such inconsistency may be due to differences in the treatment with agonists or stimuli. The previous study exposed fibroblasts to hypoxia for 48 h or to ionomycin for 24 h. The present study administered OXO for no more than 1 h and therefore the results reveal a rapid extracellular and intracellular $O_2^{\bullet-}$ production response to M_1-receptor activation (as early as in 5 min) in mouse CAMs. In addition, different cell types and species may have different responses to this Nox1 regulation during acute or chronic treatments.

Using isolated small coronary arterial preparations, we also examined the functional significance of Nox-derived extracellular $O_2^{\bullet-}$ in CD38/cADPR-mediated coronary arterial response to agonists. It was demonstrated that isolated small coronary arteries from CD38-deficient mice or from $CD38^{+/+}$ mice with inhibition of cADPR signaling lacked OXO-induced vasoconstriction. This provides strong evidence that CD38/cADPR signaling is essential for the coronary arterial constrictor response to OXO. Nox1 or Nox4 siRNA can disrupt the assembly of Nox1 or Nox4 with cytosolic NAD(P)H oxidase subunits to form an integrated enzyme causing failure of NAD(P)H oxidase activation. This study demonstrated that Nox1 or Nox4 siRNA substantially blocked OXO-induced vasoconstriction in $CD38^{+/+}$ coronary arteries, suggesting that generation of both extracellular and intracellular $O_2^{\bullet-}$ is involved in OXO-induced vasoconstriction. However, in $CD38^{-/-}$ coronary arteries, Nox1 or Nox4 siRNA had no further effect on OXO-induced vasoconstriction. This suggests that CD38 deficiency or cADPR signaling blockade inhibits OXO-induced vasoconstriction by a mechanism similar to that of Nox1 or Nox4 siRNA, namely, inhibition of NAD(P)H oxidase. With respect to the mechanism by which Nox-derived ROS mediate vasoconstriction, we previously demonstrated that extracellularly produced $O_2^{\bullet-}$ activated cADPR production and thereby mobilized intracellular Ca^{2+} from the SR, which produced or enhanced coronary vasoconstriction [15,21]. In addition, we also found that intracellular $O_2^{\bullet-}$ increase may directly enhance ryanodine receptor activity on the SR and thereby increase the Ca^{2+} release response, resulting in enhanced vasoconstriction [15,21].

In summary, this study demonstrated that during M_1-receptor activation, CD38 is essential for intracellular $O_2^{\bullet-}$ production via cADPR/Ca^{2+}-mediated activation of Nox4. Moreover,Nox1-derived extracellular $O_2^{\bullet-}$ enhances cADPR/Ca^{2+}-mediated intracellular $O_2^{\bullet-}$ production in CAMs and vasoconstriction in coronary arteries. These data provide new insights into the regulation of NAD(P)H oxidase-mediated $O_2^{\bullet-}$ production by the CD38/cADPR signaling pathway.

References

[1] Griendling, K. K.; Sorescu, D.; Ushio-Fukai, M. NAD(P)H oxidase: role in cardiovascular biology and disease. *Circ. Res.* **86:**494–501; 2000.
[2] Mohazzab, K. M.; Kaminski, P. M.; Wolin, M. S. NADH oxidoreductase is a major source of superoxide anion in bovine coronary artery endothelium. *Am. J. Physiol.* **266:**H2568–H2572; 1994.

[3] Yi, X. Y.; Li, V. X.; Zhang, F.; Yi, F.; Matson, D. R.; Jiang, M. T.; Li, P. L. Characteristics and actions of NAD(P)H oxidase on the sarcoplasmic reticulum of coronary artery smooth muscle. *Am. J. Physiol. Heart Circ. Physiol.* **290:**H1136–H1144; 2006.
[4] Griendling, K. K.; Ushio-Fukai, M. NADH/NADPH oxidase and vascular function. *Trends Cardiovasc. Med.* **7:**301–307; 1997.
[5] Hilenski, L. L.; Clempus, R. E.; Quinn, M. T.; Lambeth, J. D.; Griendling, K. K. Distinct subcellular localizations of Nox1 and Nox4 in vascular smooth muscle cells. *Arterioscler. Thromb. Vasc. Biol.* **24:**677–683; 2004.
[6] Li, Q.; Harraz, M. M.; Zhou, W.; Zhang, L. N.; Ding, W.; Zhang, Y.; Eggleston, T.; Yeaman, C.; Banfi, B.; Engelhardt, J. F. Nox2 and Rac1 regulate H_2O_2-dependent recruitment of TRAF6 to endosomal interleukin-1 receptor complexes. *Mol. Cell. Biol.* **26:**140–154; 2006.
[7] Wu, R. F.; Xu, Y. C.; Ma, Z.; Nwariaku, F. E.; Sarosi Jr., G. A.; Terada, L. S. Subcellular targeting of oxidants during endothelial cell migration. *J. Cell Biol.* **171:**893–904; 2005.
[8] Zhang, A. Y.; Yi, F.; Zhang, G.; Gulbins, E.; Li, P. L. Lipid raft clustering and redox signaling platform formation in coronary arterial endothelial cells. *Hypertension* **47:**74–80; 2006.
[9] Zhang, G.; Zhang, F.; Muh, R.; Yi, F.; Chalupsky, K.; Cai, H.; Li, P. L. Autocrine/paracrine pattern of superoxide production through NAD(P)H oxidase in coronary arterial myocytes. *Am. J. Physiol. Heart Circ. Physiol.* **292:**H483–H495; 2007.
[10] Zhang, F.; Jin, S.; Yi, F.; Xia, M.; Dewey, W. L.; Li, P. L. Local production of O_2^- by NAD(P)H oxidase in the sarcoplasmic reticulum of coronary arterial myocytes: cADPR-mediated Ca^{2+} regulation. *Cell. Signal.* **20:**637–644; 2008.
[11] Jin, S.; Yi, F.; Li, P. L. Contribution of lysosomal vesicles to the formation of lipid raft redox signaling platforms in endothelial cells. *Antioxid. Redox Signal.* **9:** 1417–1426; 2007.
[12] Das, D. K.; Maulik, N.; Sato, M.; Ray, P. S. Reactive oxygen species function as second messenger during ischemic preconditioning of heart. *Mol. Cell. Biochem.* **196:**59–67; 1999.
[13] Cancela, J. M. Specific Ca2 + signaling evoked by cholecystokinin and acetylcholine: the roles of NAADP, cADPR, and IP3. *Annu. Rev. Physiol.* **63:**99–117; 2001.
[14] Ge, Y.; Jiang, W.; Gan, L.; Wang, L.; Sun, C.; Ni, P.; Liu, Y.; Wu, S.; Gu, L.; Zheng, W.; Lund, F. E.; Xin, H. B. Mouse embryonic fibroblasts from CD38 knockout mice are resistant to oxidative stresses through inhibition of reactive oxygen species production and Ca^{2+} overload. *Biochem. Biophys. Res. Commun.* **399:**167–172; 2010.
[15] Zhang, A. Y.; Yi, F.; Teggatz, E. G.; Zou, A. P.; Li, P. L. Enhanced production and action of cyclic ADP-ribose during oxidative stress in small bovine coronary arterial smooth muscle. *Microvasc. Res.* **67:**159–167; 2004.
[16] Jia, S. J.; Jin, S.; Zhang, F.; Yi, F.; Dewey, W. L.; Li, P. L. Formation and function of ceramide-enriched membrane platforms with CD38 during M1-receptor stimulation in bovine coronary arterial myocytes. *Am. J. Physiol. Heart Circ. Physiol.* **295:** H1743–H1752; 2008.
[17] Teng, B.; Ansari, H. R.; Oldenburg, P. J.; Schnermann, J.; Mustafa, S. J. Isolation and characterization of coronary endothelial and smooth muscle cells from A1 adenosine receptor-knockout mice. *Am. J. Physiol. Heart Circ. Physiol.* **290:**H1713–H1720; 2006.
[18] Chen, C. S. Phorbol ester induces elevated oxidative activity and alkalization in a subset of lysosomes. *BMC Cell Biol.* **3:**21; 2002.
[19] Jin, S.; Zhang, Y.; Yi, F.; Li, P. L. Critical role of lipid raft redox signaling platforms in endostatin-induced coronary endothelial dysfunction. *Arterioscler. Thromb. Vasc. Biol.* **28:**485–490; 2008.
[20] Chalupsky, K.; Cai, H. Endothelial dihydrofolate reductase: critical for nitric oxide bioavailability and role in angiotensin II uncoupling of endothelial nitric oxide synthase. *Proc. Natl. Acad. Sci. U. S. A.* **102:**9056–9061; 2005.
[21] Grynkiewicz, G.; Poenie, M.; Tsien, R. Y. A new generation of Ca^{2+} indicators with greatly improved fluorescence properties. *J. Biol. Chem.* **260:**3440–3450; 1985.
[22] Ohta, S.; Suzuki, K.; Tachibana, K.; Yamada, G. Microbubble-enhanced sonoporation: efficient gene transduction technique for chick embryos. *Genesis* **37:** 91–101; 2003.
[23] Taniyama, Y.; Tachibana, K.; Hiraoka, K.; Namba, T.; Yamasaki, K.; Hashiya, N.; Aoki, M.; Ogihara, T.; Yasufumi, K.; Morishita, R. Local delivery of plasmid DNA into rat carotid artery using ultrasound. *Circulation* **105:**1233–1239; 2002.
[24] Zhang, F.; Zhang, G.; Zhang, A. Y.; Koeberl, M. J.; Wallander, E.; Li, P. L. Production of NAADP and its role in Ca^{2+} mobilization associated with lysosomes in coronary arterial myocytes. *Am. J. Physiol. Heart Circ. Physiol.* **291:**H274–H282; 2006.
[25] Lui, A. H.; McManus, B. M.; Laher, I. Endothelial and myogenic regulation of coronary artery tone in the mouse. *Eur. J. Pharmacol.* **410:**25–31; 2000.
[26] Brandin, L.; Bergstrom, G.; Manhem, K.; Gustafsson, H. Oestrogen modulates vascular adrenergic reactivity of the spontaneously hypertensive rat. *J. Hypertens.* **21:** 1695–1702; 2003.
[27] Bund, S. J.; Lee, R. M. Arterial structural changes in hypertension: a consideration of methodology, terminology and functional consequence. *J. Vasc. Res.* **40:** 547–557; 2003.
[28] Han, W. Q.; Xia, M.; Zhang, C.; Zhang, F.; Xu, M.; Li, N. J.; Li, P. L. SNARE-mediated rapid lysosome fusion in membrane raft clustering and dysfunction of bovine coronary arterial endothelium. *Am. J. Physiol. Heart Circ. Physiol.* **301:**H2028–H2037; 2011.
[29] Li, N.; Chen, L.; Yi, F.; Xia, M.; Li, P. L. Salt-sensitive hypertension induced by decoy of transcription factor hypoxia-inducible factor-1alpha in the renal medulla. *Circ. Res.* **102:**1101–1108; 2008.
[30] Yi, F. X.; Zhang, A. Y.; Campbell, W. B.; Zou, A. P.; Van Breemen, C.; Li, P. L. Simultaneous in situ monitoring of intracellular Ca^{2+} and NO in endothelium of coronary arteries. *Am. J. Physiol. Heart Circ. Physiol.* **283:**H2725–H2732; 2002.
[31] Lassegue, B.; Clempus, R. E. Vascular NAD(P)H oxidases: specific features, expression, and regulation. *Am. J. Physiol. Regul. Integr. Comp. Physiol.* **285:**R277–R297; 2003.
[32] Berruet, L.; Muller-Steffner, H.; Schuber, F. Occurrence of bovine spleen CD38/NAD^+ glycohydrolase disulfide-linked dimers. *Biochem. Mol. Biol. Int.* **46:** 847–855; 1998.
[33] Munshi, C.; Baumann, C.; Levitt, D.; Bloomfield, V. A.; Lee, H. C. The homo-dimeric form of ADP-ribosyl cyclase in solution. *Biochim. Biophys. Acta* **1388:**428–436; 1998.
[34] Caborn, D. N.; Coen, M.; Neef, R.; Hamilton, D.; Nyland, J.; Johnson, D. L. Quadrupled semitendinosus-gracilis autograft fixation in the femoral tunnel: a comparison between a metal and a bioabsorbable interference screw. *Arthroscopy* **14:**241–245; 1998.